

Building defect conformal field theory from the Sachdev-Ye-Kitaev interactions

Yang Ge and Shao-Kai Jian*

Department of Physics and Engineering Physics, Tulane University, New Orleans, Louisiana 70118, USA

(Dated: March 28, 2024)

The coupling between defects and extended critical degrees of freedom gives rise to the intriguing theory known as defect conformal field theory (CFT). In this work, we introduce a novel family of boundary and interface CFTs by coupling N Majorana chains with SYK $_q$ interactions at the defect. Our analysis reveals that the interaction with $q = 2$ constitutes a new marginal defect. Employing a versatile saddle point method, we compute unique entanglement characterizations, including the g -function and effective central charge, of the defect CFT. Furthermore, we analytically evaluate the transmission coefficient using CFT techniques. Surprisingly, the transmission coefficient deviates from the universal relation with the effective central charge across the defect at the large N limit, suggesting that our defect CFT extends beyond all known examples of Gaussian defect CFT.

Introduction.—Understanding the defect or boundary conformal field theory (CFT) holds significant implications across various domains of theoretical physics [1–3]. In condensed matter physics, defect CFT provides a powerful framework for deciphering critical behaviors of complex materials characterized by boundaries, interfaces, and defects. Any real-world materials possess boundaries, necessitating the study of boundary CFT. In particular, boundary phenomena host the most interesting physics in symmetry-protected topological phases [4, 5]. Additionally, within the framework of string theory, defect CFT naturally emerges in the study of D-branes [6, 7], offering insights on topics including brane intersections and holographic correspondences [8–10] between gravitational theories and boundary CFTs [11, 12].

Transmission and reflection are crucial characterizations of interfaces in CFTs [13, 14]. Interactions can render defects relevant or irrelevant, leading to asymptotic behaviors where defects become completely reflective or transmitting. In 2D free massless fermion theories, it was discovered that defects can be marginal, resulting in partial transmission and reflection [14–19].

On the other hand, entanglement emerges as a useful characterization of many-body wavefunctions [20–23]. One of the most successful ways to quantify the many-body entanglement is through the Rényi entropy [24]: given a pure many-body wavefunction $|\Psi\rangle$ and a bipartition $A \cup B$, the Rényi entropy is $S_n(A) = \frac{1}{1-n} \log \text{Tr}[\rho_A^n]$ with $\rho_A = \text{Tr}_B[\rho]$ being the reduced density matrix on A . While the entanglement entropy in a CFT is closely related to its central charge [25, 26], it can be altered by the presence of defects. In this context, boundary entropy, or the g -function [27], characterizes ground state degeneracy in the presence of boundaries or defects and serves as a universal property. More explicitly, boundary conditions contribute to the free energy by a constant independent of its system size L when L is large. Moreover, for marginal defects in free fermion CFTs, the entanglement entropy or Rényi entropy across the defect is captured by an effective central charge, which exhibits a universal function of the transmission coefficient [28–35].

While simple defects in free CFTs are well understood, the Sachdev-Ye-Kitaev (SYK) model [36–39], a zero-dimensional quantum mechanical model, presents a unique

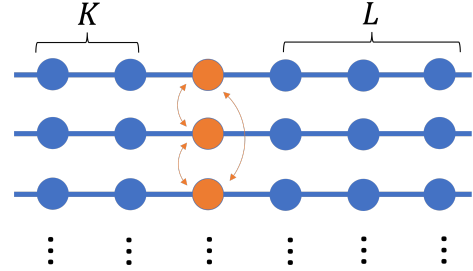


FIG. 1. Illustration of the model. The dots denote each site of the Majorana chain. There are N free Majorana chains, that are coupled via SYK interactions at the orange site. We refer to this site as the SYK site. Open boundary condition is assumed and the number of sites to the left (right) of the SYK site is K (L).

and solvable candidate for defects, beyond all known examples. Initially introduced as a solvable toy model with intriguing properties akin to black holes, the SYK model has found generalizations producing solvable models in various fields, including non-Fermi liquid behavior [40–45], thermalization [46–52], and non-Hermitian physics [53–57]. The interplay between the SYK model and CFTs has been studied in the context of black hole evaporation [58–60]. However, the joint system, where SYK acts as a defect [61–63], remains relatively unexplored. Key questions include constructing a defect CFT from the SYK model and identifying unique characterizations of such a defect CFT.

In this paper, we build boundary or defect CFTs by coupling N Majorana chains with SYK $_q$ -type interactions at the defect, as illustrated in Fig. 1. We show that the interaction with $q > 2$ is irrelevant, whereas for $q = 2$ it is marginal. We develop a saddle-point method to investigate the Rényi entropy of various bipartitions in the joint system. In a symmetric island bipartition, the g -function is shown to be one. Furthermore, we computed the Rényi entropy across the SYK defect and extract a continuous effective central charge on the SYK interaction strength. Finally, we analytically calculate the transmission coefficient across the SYK defect, which deviates from the universal relation between the Rényi entropy and the transmission. This deviation suggests that our defect CFT is distinguished from all known examples of Gaussian

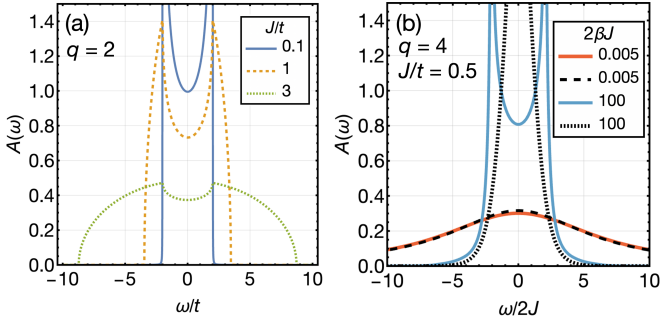


FIG. 2. Local spectral functions at the SYK_q site, on infinite chains for $q=2, 4$, at different interaction strength and temperature. (a) The SYK₂-site spectral weights at various J/t . They are temperature independent. (b) The temperature evolution of the spectral function at an SYK₄ site with $J/t = 0.5$. The two dashed black curves show the spectral functions of the 0+1D SYK model at $2\beta J = 0.005$ and 100. Deviation from the SYK fixed point at low temperature near zero frequency shows that the SYK₄ term is irrelevant. On infinite chains, the spectral function flow has almost settled at $2\beta J \sim 0.2$.

defect CFT, owing to the non-Gaussianity induced by the random coupling in our model [33].

Model.—We consider the Hamiltonian $H = H_{\text{CFT}} + H_1$, where H_{CFT} consists of N decoupled Majorana chains,

$$H_{\text{CFT}} = -i2t \sum_r \psi_{j,r} \psi_{j,r+1}, \quad (1)$$

and H_1 denotes the interface given by SYK interaction

$$H_1 = i^{q/2} \sum_{j_1, \dots, j_q} J_{j_1, \dots, j_q} \psi_{j_1, 0} \dots \psi_{j_q, 0}. \quad (2)$$

Here, r is the site index, and $j = 1, \dots, N$ denotes the flavor of Majorana at each site. Namely, each site has N Majorana fermions. Thus, $\psi_{j,r}$ denotes the j -th Majorana fermion at site r which satisfies $\{\psi_{j,r}, \psi_{j',r'}\} = \delta_{j,j'} \delta_{r,r'}$, and t gives the hopping amplitude between nearest-neighbor sites. The SYK_q interaction that couples different chains sits at the site $r = 0$. We refer to it as the SYK site. The interaction strength J_{j_1, \dots, j_q} is a Gaussian variable with mean zero and variance

$$\overline{J_{j_1, \dots, j_q} J_{j'_1, \dots, j'_q}} = \delta_{j_1, j'_1} \dots \delta_{j_q, j'_q} \frac{2^{q-1} J^2 (q-1)!}{N^{q-1}}. \quad (3)$$

A schematic plot of the model is in Fig. 1.

We use the G - Σ action to solve the model, where $G(\tau) = \frac{1}{N} \sum_j \langle \psi_{j,0}(\tau) \psi_{j,0}(0) \rangle$ and Σ denotes the corresponding self-energy [see Supplemental Material (SM) Sec. I for details]. Note that the bracket in G indicates both quantum and disorder averages, and τ denotes the imaginary time. In the large- N limit, the Dyson-Schwinger equations are

$$\begin{aligned} G^{-1}(i\omega_n) &= -i\omega_n - \Sigma(i\omega_n) - tR_K\left(\frac{-i\omega_n}{2t}\right) - tR_L\left(\frac{-i\omega_n}{2t}\right), \\ \Sigma(\tau) &= J^2 [2G(\tau)]^{q-1}, \end{aligned} \quad (4)$$

where $G(i\omega_n) = \int d\tau G(\tau) e^{i\omega_n \tau}$ in the Matsubara frequency domain with $\omega_n = \frac{(2n+1)\pi}{\beta}$ and β is the inverse temperature.

Here, coupling to the Majorana chains results in corrections to the self-energy in the form of ratios of the Chebyshev polynomials, $R_L(x) \equiv \frac{U_{L-1}(x)}{U_L(x)}$, where U is the Chebyshev polynomial of the second kind.

A simple scaling analysis reveals that the SYK interaction is marginal for $q=2$ and irrelevant for $q>2$, since $[J] = 1 - \frac{q}{2}$, where $[\cdot]$ denotes the scaling dimension. This is confirmed by exactly solving the model in the thermodynamic limit, $K, L \rightarrow \infty$, so that $\lim_{L \rightarrow \infty} R_L(x) = x - \sqrt{x^2 - 1}$. The local spectral function at the SYK site, $A(\omega) \equiv 2G''(\omega - i\eta)$ can be used to expand G and solve for the advanced self-energy

$$\begin{aligned} \Sigma_q''(\omega - i\eta) &= J^2 \int \left[\prod_{i=1}^{q-2} \frac{d\nu_i}{\pi} A(\nu_i) \right] A\left(\omega - \sum_{j=1}^{q-2} \nu_j\right) \\ &\quad \prod_{k=1}^{q-2} \left[n_1(\nu_k) - n_{\zeta_k} \left(\sum_{l=k}^{q-2} \nu_l - \omega \right) \right], \end{aligned} \quad (5)$$

where $\zeta_k = \text{mod}(k, 2)$, and $n_{\zeta_k}(\nu) = 1/[-(-1)^{\zeta_k+1} + e^{\beta\nu}]$ is related to the Fermi-Dirac ($\zeta_k = 1$) and Bose-Einstein ($\zeta_k = 0$) distributions (see SM Sec. II for details). Hence, the self-energy and Green's function are temperature independent in the marginal $q=2$ case, while they flow away from the SYK fixed point when $q>2$ at low temperature. This is confirmed by the exact solutions plotted in Fig. 2. The spectral function of the SYK₂ site is shown in Fig. 2(a), where it evolves continuously in J/t . The two peaks originate from the band edges of the Majorana chain, whereas the semicircle originates from the SYK site. On the other hand, for $q=4$ we compare the spectral function of the defect site with that of a decoupled SYK site in Fig. 2(b). The deviation between the two at low temperature near zero frequency demonstrates the irrelevance of the SYK₄ interaction. Consequently, we will focus on $q=2$ in the remainder of the discussion, although our formalism applies to any q .

Rényi entropy.—Sitting between two 1+1D CFTs as in Fig. 1, the SYK site constitutes a conformal defect at low energies and long wavelengths. Its conformal data are closely related to the entanglement between different parts of the system across the SYK site [28, 32, 33]. Using the replica trick and the large- N analysis, we present a method [51, 60, 64] to conveniently extract the Rényi entanglement entropy for an arbitrary bipartition as depicted in Fig. 3(a). We compute the second Rényi entropy below as an example, which is later used to obtain the g -function and the effective central charge.

The second Rényi entropy of region A is given by its reduced density matrix,

$$S_2 = -\log \text{Tr}_A [(\text{Tr}_B \rho)^2] = -\log \frac{Z_{(2)}}{Z^2}. \quad (6)$$

The replica trick conducts the partial trace with different imaginary-time boundary conditions in regions A and B [25, 51, 60]. Here $Z_{(2)}$ denotes a two-replica path integral with a twisted boundary condition in region B , while Z is the path integral corresponding to the thermal density matrix

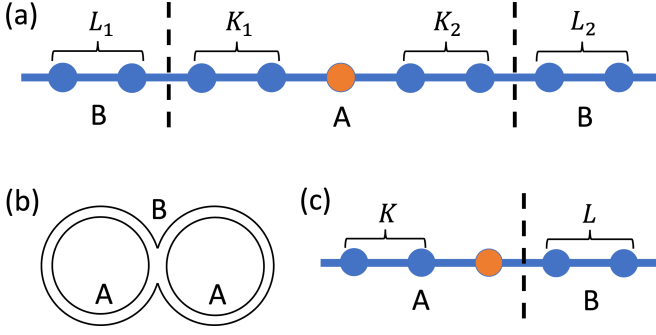


FIG. 3. (a) A generic bipartition of 1+1D open chains. For simplicity, a single chain is plotted, which nevertheless should be understood as N chains. The orange site is the SYK site. (b) The imaginary time contour for the second Rényi entropy. The fermionic field in a closed contour satisfies the conventional anti-periodic boundary condition, that leads to the fermionic Matsubara frequency. Region B has the twisted boundary condition threading the two replicas. (c) Setup for the interface CFT induced at the SYK site, where $L_1 = K_2 = 0$.

$\rho := e^{-\beta H}/Z$. Boundary conditions of the replica fields differ between regions A and B ,

$$\begin{aligned} \psi_j^{(1)}(\beta) &= -\psi_j^{(1)}(0), & \psi_j^{(2)}(\beta) &= -\psi_j^{(2)}(0), & j \in A, \\ \psi_j^{(1)}(\beta) &= \psi_j^{(2)}(0), & \psi_j^{(2)}(\beta) &= -\psi_j^{(1)}(0), & j \in B. \end{aligned} \quad (7)$$

where the superscripts 1 and 2 denote the two replicas. The imaginary time contour for $Z_{(2)}$ is depicted in Fig. 3(b). We join the two replicas into $\tau \in (0, 2\beta)$, so that the fields can be expanded in Matsubara frequencies $\omega_n^{(1)} = \omega_n^{(2)} = (2n+1)\pi/\beta$ in region A , and $\Omega_n = (2n+1)\pi/2\beta$ in region B ,

$$\psi_j(\tau) = \begin{cases} \frac{1}{\sqrt{\beta}} \sum_n \psi_j(i\omega_n^{(1)}) e^{-i\omega_n^{(1)}\tau}, & j \in A, \tau < \beta, \\ \frac{1}{\sqrt{\beta}} \sum_n \psi_j(i\omega_n^{(2)}) e^{-i\omega_n^{(2)}\tau}, & j \in A, \tau > \beta, \\ \frac{1}{\sqrt{2\beta}} \sum_n \psi_j(i\Omega_n) e^{-i\Omega_n\tau}, & j \in B. \end{cases} \quad (8)$$

At large- N , we compute $Z_{(2)}$ by solving for the Green's function $G_{(2)}$ at the SYK site, and then substitute it into the twisted action. (See SM Sec. III for details.) At the partition interface, the twist operator σ , defined below, breaks the time-translational symmetry. The resulting saddle point solution is

$$\begin{aligned} G_{(2)}^{-1}(i\omega_m^{(a)}, i\omega_n^{(b)}) &= -i\omega_n^{(a)} \delta_{ab} \delta_{mn} - \Sigma_{(2)}(i\omega_m^{(a)}, i\omega_n^{(b)}) \\ &\quad - t(\mathbf{D}_{K_1, L_1})_{mn}^{ab} - t(\mathbf{D}_{K_2, L_2})_{mn}^{ab}, \\ \Sigma_{(2)}(\tau_1, \tau_2) &= J^2 [2G_{(2)}(\tau_1, \tau_2)]^{q-1}. \end{aligned} \quad (9)$$

Here the self-energy due to the rest of the Majorana chain is given by

$$\begin{aligned} \mathbf{D}_{0,L} &= \sigma R_L \left(\frac{-i\Omega}{2t} \right) \sigma^\dagger, \\ \mathbf{D}_{K,L} &= \left(-\frac{i\omega}{t} - \mathbf{D}_{K-1,L} \right)^{-1}, \end{aligned} \quad (10)$$

where we have defined the Matsubara frequency matrices

$$\begin{aligned} \omega &= \text{diag}(\omega_1^{(1)}, \omega_2^{(1)}, \dots, \omega_1^{(2)}, \omega_2^{(2)}, \dots), \\ \Omega &= \text{diag}(\Omega_1, \Omega_2, \dots). \end{aligned} \quad (11)$$

[See SM Eq. (S34) for a general formula of \mathbf{D} .] The twist operator σ transforms fields across the partition, which in frequency space is

$$\sigma(i\omega_m^{(a)}, i\Omega_n) = \begin{cases} \int_0^\beta \frac{d\tau}{\sqrt{2\beta}} \exp\{i[\omega_m^{(a)} - \Omega_n]\tau\}, & a = 1, \\ \int_\beta^{2\beta} \frac{d\tau}{\sqrt{2\beta}} \exp\{i[\omega_m^{(a)} - \Omega_n]\tau\}, & a = 2. \end{cases} \quad (12)$$

Following (6), $S_2 = I_{(2)} - 2I$ is the difference between the actions corresponding to $Z_{(2)}$ and Z . The expression simplifies after subtracting the zero S_2 when A and B are decoupled. Denote the actions in a decoupled system by \check{I} , we arrive at the formula for the second Rényi entropy between A and B ,

$$\begin{aligned} \frac{S_2}{N} &= \frac{I_{(2)}}{N} - \frac{2I}{N} - \left(\frac{\check{I}_{(2)}}{N} - \frac{2\check{I}}{N} \right) \\ &= -\frac{1}{2} \text{Tr} \log [G_{(2)}^{-1} \check{G}] + J^2 \left(\frac{1}{4q} - \frac{1}{4} \right) \\ &\quad \times \int d\tau_1 d\tau_2 \{ [2\check{G}(\tau_1, \tau_2)]^q - [2G_{(2)}(\tau_1, \tau_2)]^q \} \\ &\quad + \sum_{s=1,2} \frac{1}{2} \text{Tr} \log \left[\frac{1 - R_{L_s} \left(\frac{-i\omega}{2t} \right) R_{K_s} \left(\frac{-i\omega}{2t} \right)}{1 - \sigma R_{L_s} \left(\frac{-i\Omega}{2t} \right) \sigma^\dagger R_{K_s} \left(\frac{-i\omega}{2t} \right)} \right], \end{aligned} \quad (13)$$

where $\check{G} = G \otimes \mathbf{1}_2$ is the Green's function for Z , i.e. (4) with $K \rightarrow L_1 + K_1$ and $L \rightarrow L_2 + K_2$, replicated diagonally in the replica space. The last line is simply the entanglement between free Majorana chains with uniform nearest-neighbor hoppings.

Energy defect.—Two distinct bipartitions for the Rényi entropy that reveal universal conformal data have been considered in the literature: i) where the defect is located deep inside one subsystem, say A ; ii) where the bipartition between two subsystems A and B is located at or near the defect. The first bipartition reveals the g -function via a folding trick, i.e., the offset of Rényi entropy between the system with and without defect equals the boundary entropy of a folded system with doubled degrees of freedom [16, 65, 66]. In the second bipartition, the second Rényi entanglement entropy across the interface is $S_2 \sim \frac{\tilde{c}_2}{8} \log L_A$ where L_A is the size of region A (for simplicity we set $L_B = L_A$). The prefactor \tilde{c}_2 precisely defines the effective central charge, which can differ from the central charge of the bulk CFT. In free fermion CFTs, the effective central charge is a universal function of the transmission coefficient \mathcal{T} [31], i.e.,

$$\tilde{c}_2 \equiv \frac{8}{\pi^2} \arcsin^2 \sqrt{\frac{\mathcal{T}}{2}}. \quad (14)$$

Before moving on to the SYK defect, we use our path integral method to evaluate the g -function and the effective central charge for the energy defect as a warmup [15, 16, 34]. The energy defect in the Ising CFT can be modeled by replacing the SYK site by a defect bond with a distinct hopping amplitude t' [31, 34]. Since different chains do not couple with such a defect, we can instead consider $N = 1$. With a slight

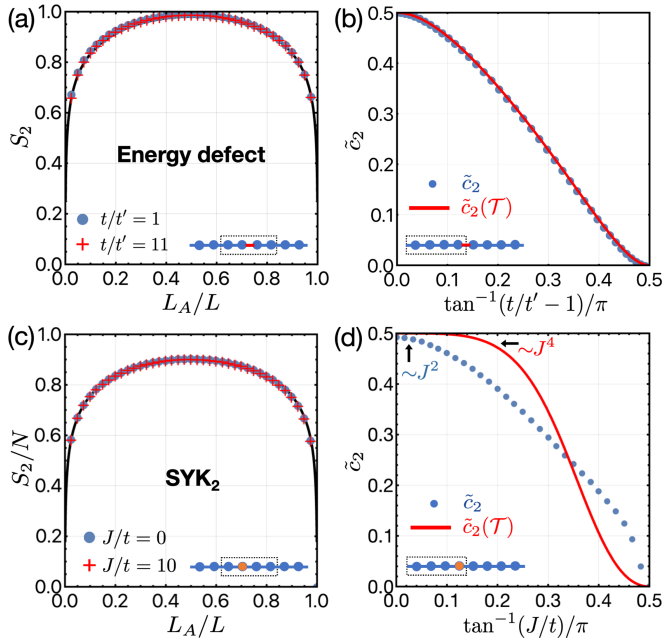


FIG. 4. The second Rényi entropy and the extracted effective central charge under different partition schemes, in the presence of (a)–(b) an energy defect with bond strength t' , and (c)–(d) SYK₂ coupling of strength J across N Majorana chains, both at the center of the chain. The setups are depicted in the insets. In (a) and (c), subsystem A is the center region. Its entropy per chain is plotted as a function of the subsystem size fraction L_A/L , varying symmetrically about the center. The black curves give the analytical dependence of S_2 on L_A/L with $c_2 = 1/2$ and $L = 4000$ [Eq. (15)]. In (b) and (d), the partition is at the defect. The extracted central charge is plotted against the defect strength, both from the logarithmic scaling of S_2 (dots) and from the transmission probability \mathcal{T} using Eq. (14) (line). Their disagreement in (d) signals non-Gaussianity.

modification, our saddle-point method can be used to evaluate the Rényi entropy of the free fermion chain with such a defect. The result is shown in Fig. 4(a)(b): Fig. 4(a) shows that $\log g = 0$ for the energy defect, and Fig. 4(b) shows the effective central charge. The effective central charge is plotted along with the exact analytical result (14), with $\sqrt{\mathcal{T}} = \frac{2}{t'/t + t/t'}$. This benchmarks our method.

g-function.—To determine the g -function for the SYK defect, we place an SYK₂ defect in the middle of region A in a symmetric setup, i.e., $L_1 = L_2$ and $K_1 = K_2$ in Fig. 3(a), and compute S_2 as the subsystem size fraction varies while the total length is fixed. Since the g -function is universal, S_2 should depend logarithmically on the size of region A , L_A , with a constant offset when $\beta \gg L$ [25, 34],

$$\frac{S_2}{N} = \frac{c_2}{4} \log \left[\frac{L}{\pi} \sin \left(\frac{\pi L_A}{L} \right) \right] + s, \quad (15)$$

such that the constant $s = \log g$ is independent of the defect strength J . Here, the factor $c_2/4$ is the sum of the equal contribution $c_2/8$ from each of the two interfaces. The universality of s is confirmed by our result in Fig. 4(c), which shows no offset between the entropy curve at different J 's [67]. This

implies that the g -function is $\log g = 0$, same as that of an energy defect.

Effective central charge.—To determine the effective central charge for the SYK defect, we partition our system at the SYK site as depicted in Fig. 3(c). The result is a defect CFT determined by the bulk free CFTs and the SYK defect [29]. The second Rényi entanglement entropy across the SYK defect is $\frac{S_2}{N} \sim \frac{c_2}{8} \log L_A$ [28, 31–33], where the factor N is due to the large- N structure of the SYK interaction. Thus, we can obtain the effective central charge \tilde{c}_2 of the defect CFT by tracking S_2 while increasing the size of the system symmetrically in A and B . The result is plotted as dots in Fig. 4(d). With increasing interaction strength, \tilde{c}_2 decreases toward zero and the two sides become decoupled. Therefore, the marginal $q = 2$ SYK interaction induces an interface CFT with a continuously tunable effective central charge. For the irrelevant cases of $q > 2$, the \tilde{c}_2 remains at $1/2$, that of a free Majorana chain or Ising CFT. A relevant coupling can reduce \tilde{c}_2 to zero at any finite J , as is formally the case of bosonic chains coupled by the SYK interaction, although the naive bosonic SYK is ill-defined and unstable [61, 68, 69]. Finite- N calculations in the SYK₂ case give the same qualitative result.

Transmission and reflection.—In addition to the entanglement properties, the defect CFT is further characterized by the transmission and reflection probabilities, \mathcal{T} and $\mathcal{R} = 1 - \mathcal{T}$, across the defect [14, 17]. To utilize the CFT technique, we take the continuum limit using the low-energy chiral modes at the two Fermi momenta, $k_F = 0, \pi$, where the lattice constant is set to 1. These modes are $\psi_{L,R}(x) \sim \int_{k \sim 0, \pi} e^{-ikx} \psi(k) dk$. The interaction strength in the continuum model becomes $\tilde{J} \equiv J/t$. The continuum Green's function can be directly solved and used to extract the stress-energy tensor (see SM Sec. IV). For a conformal defect, \mathcal{T} can be derived from the holomorphic and antiholomorphic components of the stress-energy tensor, T and \bar{T} , at two sides of the defect [14]. With the defect at $x = 0$,

$$\begin{aligned} \mathcal{T} &= \lim_{x \rightarrow \infty} \frac{\langle T(x)T(-x) + \bar{T}(x)\bar{T}(-x) \rangle}{\langle [T(x) + \bar{T}(-x)][\bar{T}(x) + T(-x)] \rangle} \\ &= \frac{2}{3 + \tilde{J}^2 - \sqrt{1 + 2\tilde{J}^2}}. \end{aligned} \quad (16)$$

Notice that in deriving this expression, we used a coarse graining to obtain a continuous field theory. While the coarse graining naturally asserts $\tilde{J} = J/t$, the exact relation between the UV parameters J , t and the CFT parameter \tilde{J} is not clear in general. Still, we expect $\tilde{J} = J/t$ to hold when $\tilde{J} \ll 1$. A detailed discussion on this issue is given in the SM Sec. V. If the transmission coefficient in (16) and the relation in (14) are used to determine the effective central charge \tilde{c}_2 , the result will differ significantly from the central charge \tilde{c}_2 extracted from the scaling of S_2 even at $\tilde{J} \ll 1$. In particular, for small \tilde{J} , the entanglement scaling from both numerics and analytics implies a decrease by \tilde{J}^2 , while the result from transmission coefficient decreases by \tilde{J}^4 , as can be expected from expanding (13) and (16), respectively. The disagreement signifies the

deviation from the Gaussian defect due to the disorder averaging of SYK₂, even though each random realization is non-interacting.

Concluding remarks.—We have presented a novel family of boundary and defect CFTs built from the SYK interaction coupling 1+1D systems giving rise to a tunable effective central charge. Based on path integral and functional determinant, we developed a versatile method to compute the (conformal) data of defects embedded in 1+1D. Our method can adopt arbitrary partitioning of the system and go to low temperature and large system sizes at very low cost. It can be extended to 1+1D systems with different boundary conditions, next-nearest-neighbor hoppings, etc. With this method, we have evaluated the boundary entropy and effective central charge of the defect CFT built from the SYK interaction. Our findings suggest that it extends beyond all known examples of Gaussian defect CFT.

Acknowledgments. We thank Xiao-Yang Shen for helpful discussions on the bosonic SYK model. This work is supported by a start-up grant from Tulane University.

* sjian@tulane.edu

- [1] J. L. Cardy, Conformal invariance and surface critical behavior, *Nucl. Phys. B* **240**, 514 (1984).
- [2] J. L. Cardy, Boundary conditions, fusion rules and the verlinde formula, *Nucl. Phys. B* **324**, 581 (1989).
- [3] N. Andrei, A. Bissi, M. Buican, J. Cardy, P. Dorey, N. Drukker, J. Erdmenger, D. Friedan, D. Fursaev, A. Konechny, *et al.*, Boundary and defect CFT: open problems and applications, *J. Phys. A* **53**, 453002 (2020).
- [4] M. Z. Hasan and C. L. Kane, Colloquium: Topological insulators, *Rev. Mod. Phys.* **82**, 3045 (2010).
- [5] X.-L. Qi and S.-C. Zhang, Topological insulators and superconductors, *Rev. Mod. Phys.* **83**, 1057 (2011).
- [6] A. Recknagel and V. Schomerus, *Boundary conformal field theory and the worldsheet approach to D-branes* (Cambridge University Press, 2013).
- [7] J. Polchinski, TASI lectures on D-branes, [arXiv:hep-th/9611050](https://arxiv.org/abs/hep-th/9611050) (1996).
- [8] J. Maldacena, The large- N limit of superconformal field theories and supergravity, *Int. J. Theor. Phys.* **38**, 1113 (1999).
- [9] E. Witten, Anti de Sitter space and holography, [arXiv:hep-th/9802150](https://arxiv.org/abs/hep-th/9802150) (1998).
- [10] S. S. Gubser, I. R. Klebanov, and A. M. Polyakov, Gauge theory correlators from non-critical string theory, *Phys. Lett.* **428**, 105 (1998).
- [11] T. Takayanagi, Holographic dual of a boundary conformal field theory, *Phys. Rev. Lett.* **107**, 101602 (2011).
- [12] M. Fujita, T. Takayanagi, and E. Tonni, Aspects of Ads/BCFT, *J. High Energy Phys.* **2011** (11), 43.
- [13] C. L. Kane and M. P. A. Fisher, Transmission through barriers and resonant tunneling in an interacting one-dimensional electron gas, *Phys. Rev. B* **46**, 15233 (1992).
- [14] T. Quella, I. Runkel, and G. M. T. Watts, Reflection and transmission for conformal defects, *J. High Energy Phys.* **2007** (04), 095.
- [15] M. Oshikawa and I. Affleck, Defect lines in the Ising model and boundary states on orbifolds, *Phys. Rev. Lett.* **77**, 2604 (1996).
- [16] M. Oshikawa and I. Affleck, Boundary conformal field theory approach to the critical two-dimensional Ising model with a defect line, *Nucl. Phys. B* **495**, 533 (1997).
- [17] G. Delfino, G. Mussardo, and P. Simonetti, Scattering theory and correlation functions in statistical models with a line of defect, *Nucl. Phys. B* **432**, 518 (1994).
- [18] C. Bachas, J. de Boer, R. Dijkgraaf, and H. Ooguri, Permeable conformal walls and holography, *J. High Energy Phys.* **2002** (06), 027.
- [19] C. Bachas, I. Brunner, and D. Roggenkamp, Fusion of critical defect lines in the 2d Ising model, *J. Stat. Mech.: Theory Exp.* **2013** (08), P08008.
- [20] L. Amico, R. Fazio, A. Osterloh, and V. Vedral, Entanglement in many-body systems, *Rev. Mod. Phys.* **80**, 517 (2008).
- [21] R. Horodecki, P. Horodecki, M. Horodecki, and K. Horodecki, Quantum entanglement, *Rev. Mod. Phys.* **81**, 865 (2009).
- [22] P. Calabrese, J. Cardy, and B. Doyon, Entanglement entropy in extended quantum systems, *J. Phys. A: Math. Theor.* **42**, 500301 (2009).
- [23] J. Eisert, M. Cramer, and M. B. Plenio, Colloquium: Area laws for the entanglement entropy, *Rev. Mod. Phys.* **82**, 277 (2010).
- [24] P. Jizba and T. Arimitsu, The world according to Rényi: thermodynamics of multifractal systems, *Ann. Phys. (N. Y.)* **312**, 17 (2004).
- [25] P. Calabrese and J. Cardy, Entanglement entropy and quantum field theory, *J. Stat. Mech.* **2004**, P06002 (2004).
- [26] P. Calabrese and J. Cardy, Entanglement entropy and conformal field theory, *J. Phys. A* **42**, 504005 (2009).
- [27] I. Affleck and A. W. W. Ludwig, Universal noninteger “ground-state degeneracy” in critical quantum systems, *Phys. Rev. Lett.* **67**, 161 (1991).
- [28] K. Sakai and Y. Satoh, Entanglement through conformal interfaces, *J. High Energy Phys.* **2008** (12), 001.
- [29] V. Eisler and I. Peschel, Entanglement in fermionic chains with interface defects, *Ann. Phys. (Berlin)* **522**, 679 (2010).
- [30] P. Calabrese, M. Mintchev, and E. Vicari, Entanglement entropy of quantum wire junctions, *J. Phys. A* **45**, 105206 (2012).
- [31] I. Peschel and V. Eisler, Exact results for the entanglement across defects in critical chains, *J. Phys. A* **45**, 155301 (2012).
- [32] E. Brehm and I. Brunner, Entanglement entropy through conformal interfaces in the 2d Ising model, *J. High Energy Phys.* **2015** (9), 80.
- [33] L. Capizzi, S. Murciano, and P. Calabrese, Rényi entropy and negativity for massless dirac fermions at conformal interfaces and junctions, *J. High Energy Phys.* **2022** (8), 171.
- [34] D. Rogerson, F. Pollmann, and A. Roy, Entanglement entropy and negativity in the Ising model with defects, *J. High Energy Phys.* **2022** (6).
- [35] A. Roy and H. Saleur, Entanglement entropy in the Ising model with topological defects, *Phys. Rev. Lett.* **128**, 090603 (2022).
- [36] S. Sachdev and J. Ye, Gapless spin-fluid ground state in a random quantum Heisenberg magnet, *Phys. Rev. Lett.* **70**, 3339 (1993).
- [37] A. Kitaev, A simple model of quantum holography, *KITP strings seminar and entanglement 2015 program* (2015).
- [38] J. Maldacena and D. Stanford, Remarks on the Sachdev-Ye-Kitaev model, *Phys. Rev. D* **94**, 106002 (2016).
- [39] J. Polchinski and V. Rosenhaus, The spectrum in the Sachdev-Ye-Kitaev model, *J. High Energy Phys.* **2016** (4), 1.
- [40] D. Chowdhury, A. Georges, O. Parcollet, and S. Sachdev, Sachdev-Ye-Kitaev models and beyond: Window into non-Fermi liquids, *Rev. Mod. Phys.* **94**, 035004 (2022).
- [41] X.-Y. Song, C.-M. Jian, and L. Balents, Strongly correlated metal built from Sachdev-Ye-Kitaev models, *Phys. Rev. Lett.*

- 119**, 216601 (2017).
- [42] Z. Bi, C.-M. Jian, Y.-Z. You, K. A. Pawlak, and C. Xu, Instability of the non-Fermi-liquid state of the Sachdev-Ye-Kitaev model, *Phys. Rev. B* **95**, 205105 (2017).
- [43] S.-K. Jian, Z.-Y. Xian, and H. Yao, Quantum criticality and duality in the Sachdev-Ye-Kitaev/AdS₂ chain, *Phys. Rev. B* **97**, 205141 (2018).
- [44] D. Chowdhury, Y. Werman, E. Berg, and T. Senthil, Translationally invariant non-Fermi-liquid metals with critical Fermi surfaces: Solvable models, *Phys. Rev. X* **8**, 031024 (2018).
- [45] A. A. Patel, J. McGreevy, D. P. Arovas, and S. Sachdev, Magnetotransport in a model of a disordered strange metal, *Phys. Rev. X* **8**, 021049 (2018).
- [46] Y.-Z. You, A. W. W. Ludwig, and C. Xu, Sachdev-Ye-Kitaev model and thermalization on the boundary of many-body localized fermionic symmetry-protected topological states, *Phys. Rev. B* **95**, 115150 (2017).
- [47] S.-K. Jian and H. Yao, Solvable Sachdev-Ye-Kitaev models in higher dimensions: From diffusion to many-body localization, *Phys. Rev. Lett.* **119**, 206602 (2017).
- [48] J. Sonner and M. Vielma, Eigenstate thermalization in the Sachdev-Ye-Kitaev model, *J. High Energy Phys.* **2017** (11), 149.
- [49] Y. Gu, A. Lucas, and X.-L. Qi, Spread of entanglement in a Sachdev-Ye-Kitaev chain, *J. High Energy Phys.* **2017** (9), 120.
- [50] A. M. García-García, B. Loureiro, A. Romero-Bermúdez, and M. Tezuka, Chaotic-integrable transition in the Sachdev-Ye-Kitaev model, *Phys. Rev. Lett.* **120**, 241603 (2018).
- [51] C. Liu, X. Chen, and L. Balents, Quantum entanglement of the Sachdev-Ye-Kitaev models, *Phys. Rev. B* **97**, 245126 (2018).
- [52] X. Dai, S.-K. Jian, and H. Yao, Global phase diagram of the one-dimensional Sachdev-Ye-Kitaev model at finite N , *Phys. Rev. B* **100**, 235144 (2019).
- [53] C. Liu, P. Zhang, and X. Chen, Non-unitary dynamics of Sachdev-Ye-Kitaev chain, *SciPost Phys.* **10**, 048 (2021).
- [54] P. Zhang, S.-K. Jian, C. Liu, and X. Chen, Emergent replica conformal symmetry in non-Hermitian SYK₂ chains, *Quantum* **5**, 579 (2021).
- [55] S.-K. Jian, C. Liu, X. Chen, B. Swingle, and P. Zhang, Measurement-induced phase transition in the monitored Sachdev-Ye-Kitaev model, *Phys. Rev. Lett.* **127**, 140601 (2021).
- [56] A. M. García-García, Y. Jia, D. Rosa, and J. J. M. Verbaarschot, Replica symmetry breaking in random non-Hermitian systems, *Phys. Rev. D* **105**, 126027 (2022).
- [57] A. M. García-García, Y. Jia, D. Rosa, and J. J. M. Verbaarschot, Dominance of replica off-diagonal configurations and phase transitions in a PT symmetric Sachdev-Ye-Kitaev model, *Phys. Rev. Lett.* **128**, 081601 (2022).
- [58] G. Penington, S. H. Shenker, D. Stanford, and Z. Yang, Replica wormholes and the black hole interior, *J. High Energy Phys.* **2022** (3), 205.
- [59] A. Almheiri, T. Hartman, J. Maldacena, E. Shaghoulian, and A. Tajdini, Replica wormholes and the entropy of hawking radiation, *J. High Energy Phys.* **2020** (5), 13.
- [60] Y. Chen, X.-L. Qi, and P. Zhang, Replica wormhole and information retrieval in the SYK model coupled to Majorana chains, *J. High Energy Phys.* **2020** (6), 121.
- [61] X.-Y. Shen, Long range SYK model and boundary SYK model, *arXiv:2308.12598* (2023).
- [62] Q. Gao, P. Zhang, and X. Chen, Information scrambling in free fermion systems with a sole interaction, *arXiv:2310.07043* (2023).
- [63] Q. Gao, T. Zhou, P. Zhang, and X. Chen, Scrambling transition in free fermion systems induced by a single impurity, *arXiv:2403.03457* (2024).
- [64] S. Shao and Y. Komijani, Towards entanglement entropy of random large- N theories, *Phys. Rev. D* **109**, 016015 (2024).
- [65] H. Saleur, Lectures on non perturbative field theory and quantum impurity problems, in *Aspects topologiques de la physique en basse dimension. Topological aspects of low dimensional systems*, edited by A. Comtet, T. Jolicœur, S. Ouvry, and F. David (Springer, Berlin, Heidelberg, 1999).
- [66] M. Gutperle and J. D. Miller, A note on entanglement entropy for topological interfaces in RCFTs, *J. High Energy Phys.* **2016** (4), 176.
- [67] A J -independent offset is added to the analytical curve in Fig. 4(c) to match the result at $J = 0$. This offset comes from the imperfect mirror symmetry in even-length Majorana chains coupled at the SYK site, as seen in the insets of Fig. 4. In contrast, no offset to the logarithm is needed for the energy defect in Fig. 4(a).
- [68] J. Murugan, D. Stanford, and E. Witten, More on supersymmetric and 2d analogs of the SYK model, *J. High Energy Phys.* **2017** (8), 146.
- [69] J. Liu, E. Perlmutter, V. Rosenhaus, and D. Simmons-Duffin, d -dimensional SYK, AdS loops, and $6j$ symbols, *J. High Energy Phys.* **2019** (3), 52.
- [70] R. K. Mallik, The inverse of a tridiagonal matrix, *Linear Algebra Appl.* **325**, 109 (2001).
- [71] A. Altland and B. D. Simons, *Condensed Matter Field Theory*, 2nd ed. (Cambridge University Press, Cambridge, 2010).
- [72] X. Zhang, *Matrix Analysis and Applications*, 2nd ed. (Tsinghua University Press, 2013).

SUPPLEMENTAL MATERIAL

I. DERIVATION OF THE LARGE- N ACTION

The model is given by the Hamiltonian $H = H_{\text{CFT}} + H_1$, where H_{CFT} consists of N decoupled Majorana chains,

$$H_{\text{CFT}} = -i2t \sum_r \psi_{j,r} \psi_{j,r+1}, \quad (\text{S1})$$

and H_1 denotes the interface given by SYK interaction

$$H_1 = i^{q/2} \sum_{j_1, \dots, j_q} J_{j_1, \dots, j_q} \psi_{j_1, 0} \dots \psi_{j_q, 0}. \quad (\text{S2})$$

Here, r is the site index, and $j = 1, \dots, N$ denotes the flavor of Majorana at each site. Namely, each site has N Majorana fermions. $\psi_{j,r}$ denotes j -th Majorana fermion at site r , $\{\psi_{j,r}, \psi_{j',r'}\} = \delta_{j,j'} \delta_{r,r'}$. t is the hopping amplitude between the nearest-neighbor sites. The SYK interaction that couples different chains exists at the site $r = 0$. We refer to it as the SYK site.

The interaction strength J_{j_1, \dots, j_q} is a Gaussian variable with mean zero and variance

$$\overline{J_{j_1, \dots, j_q} J_{j'_1, \dots, j'_q}} = \delta_{j_1, j'_1} \dots \delta_{j_q, j'_q} \frac{2^{q-1} J^2 (q-1)!}{N^{q-1}}. \quad (\text{S3})$$

After integrating over the Gaussian distributed interaction, the action reads

$$-I = -\frac{1}{2} \sum_{j, r_1, r_2} \int d\tau \psi_{j, r_1}(\tau) (\partial_\tau \delta_{r_1, r_2} - i t h_{r_1, r_2}) \psi_{j, r_2}(\tau) + \frac{N J^2}{4q} \int d\tau_1 d\tau_2 \left(2 \frac{1}{N} \sum_j \psi_{j, 0}(\tau_1) \psi_{j, 0}(\tau_2) \right)^q, \quad (\text{S4})$$

where the SYK interaction couples different chains at site $r = 0$, and $h_{r_1, r_2} = \delta_{r_2, r_1+1} - \delta_{r_2, r_1-1}$ is the hopping matrix. We introduce bilocal fields $G(\tau_1, \tau_2)$ and $\Sigma(\tau_1, \tau_2)$ to simplify the action,

$$\begin{aligned} -I &= -\frac{1}{2} \sum_{j, r_1, r_2} \int d\tau_1 d\tau_2 \psi_{j, r_1}(\tau_1) [(\partial_{\tau_1} \delta_{r_1, r_2} - i t h_{r_1, r_2}) \delta(\tau_1 - \tau_2) - \delta_{r_1, 0} \delta_{r_2, 0} \Sigma(\tau_1, \tau_2)] \psi_{j, r_2}(\tau_2) \\ &\quad - \frac{N}{2} \int d\tau_1 d\tau_2 G(\tau_1, \tau_2) \Sigma(\tau_1, \tau_2) + \frac{N J^2}{4q} \int d\tau_1 d\tau_2 [2G(\tau_1, \tau_2)]^q. \end{aligned} \quad (\text{S5})$$

It is not hard to check that, by integrating over G and Σ , this reduces to the fermionic action. Now the action is only quadratic in terms of Majorana fermions, so we can integrate them out to get

$$\begin{aligned} -\frac{I}{N} &= \frac{1}{2} \log \det [(\partial_{\tau_1} \delta_{r_1, r_2} - i t h_{r_1, r_2}) \delta(\tau_1 - \tau_2) - \delta_{r_1, 0} \delta_{r_2, 0} \Sigma(\tau_1, \tau_2)] \\ &\quad - \frac{1}{2} \int d\tau_1 d\tau_2 G(\tau_1, \tau_2) \Sigma(\tau_1, \tau_2) + \frac{J^2}{4q} \int d\tau_1 d\tau_2 (2G(\tau_1, \tau_2))^q. \end{aligned} \quad (\text{S6})$$

The determinant involves matrices whose indices range over the imaginary time and the lattice sites. Since the action has a large- N structure, we can implement a saddle point analysis. The Schwinger-Dyson equations read

$$G(\tau_1, \tau_2) = (\partial_\tau - \Sigma - i t h)_{00}^{-1}(\tau_1, \tau_2), \quad \Sigma(\tau_1, \tau_2) = J^2 [2G(\tau_1, \tau_2)]^{q-1}, \quad (\text{S7})$$

where the first equation should be understood as a matrix equation. The subscript denotes $r_1 = 0, r_2 = 0$ component.

We can further simplify the action by noting that the self-energy is nontrivial only at the SYK site. We assume the solution to be time translationally symmetric, i.e., $G(\tau_1, \tau_2) = G(\tau_1 - \tau_2)$, $\Sigma(\tau_1, \tau_2) = \Sigma(\tau_1 - \tau_2)$. In this case, we can perform a Fourier transformation in the imaginary time domain, i.e.,

$$G(\tau_1, \tau_2) = \frac{1}{\beta} \sum_n e^{i\omega_n(\tau_1 - \tau_2)} G(i\omega_n), \quad \Sigma(\tau_1, \tau_2) = \frac{1}{\beta} \sum_n e^{i\omega_n(\tau_1 - \tau_2)} \Sigma(i\omega_n), \quad \omega_n = \frac{(2n+1)\pi}{\beta}. \quad (\text{S8})$$

We consider the open boundary condition for these Majorana chains. In the frequency space, the matrix inside the determinant becomes tridiagonal in the basis of $\psi_r(i\omega_n)$ at each Matsubara frequency,

$$\mathcal{M}_{rr'} = \bigoplus_n [-i\omega_n \delta_{rr'} - \Sigma(i\omega_n) \delta_{r,0} \delta_{0,r'} - i t \delta_{r+1,r'} + i t \delta_{r,r'+1}]. \quad (\text{S9})$$

The determinant of a tridiagonal matrix has a simple analytical expression [70]. Therefore, we can first evaluate the determinant at each frequency, and then take the product over all the frequencies. After a straightforward calculation, the large- N action can be simplified as

$$-\frac{I}{N} = \frac{1}{2} \log \prod_n \left[-i\omega_n - \Sigma(i\omega_n) - tR_K\left(\frac{-i\omega_n}{2t}\right) - tR_L\left(\frac{-i\omega_n}{2t}\right) \right] - \frac{1}{2} \int d\tau_1 d\tau_2 G(\tau_1, \tau_2) \Sigma(\tau_1, \tau_2) + \frac{J^2}{4q} \int d\tau_1 d\tau_2 [2G(\tau_1, \tau_2)]^q + \frac{I'}{N}. \quad (\text{S10})$$

where $R_L(x) = \frac{U_{L-1}(x)}{U_L(x)}$, and U_L is the Chebyshev polynomial of the second kind. $K-1$ and L are the number of sites to the left and the right of the SYK sites, respectively, as shown in Fig. 1. The term

$$\frac{I'}{N} = \frac{1}{2} \sum_n \log \left[t^{L+K} U_L\left(\frac{-i\omega_n}{2t}\right) U_K\left(\frac{-i\omega_n}{2t}\right) \right] \quad (\text{S11})$$

is independent of G and Σ . Varying the bilocal fields, we obtain the corresponding Schwinger-Dyson equation

$$G(i\omega_n) = \left[-i\omega_n - \Sigma(i\omega_n) - tR_K\left(\frac{-i\omega_n}{2t}\right) - tR_L\left(\frac{-i\omega_n}{2t}\right) \right]^{-1}, \quad (\text{S12})$$

$$\Sigma(\tau_1, \tau_2) = J^2 [2G(\tau_1, \tau_2)]^{q-1}. \quad (\text{S13})$$

The effect of coupling to the Majorana chain is reflected in the correction to the self-energy in the form of ratios of the Chebyshev polynomials.

II. DERIVATION OF THE GREEN'S FUNCTION AT $L = \infty$ FOR AN ARBITRARY q

Here we derive in detail the large- N Green's function and self-energy of infinitely long SYK $_q$ -coupled Majorana chains, which is Eq. (5). To proceed, we consider an infinite number of sites to the left and right of the SYK point, i.e., $L, K \rightarrow \infty$. Observing that

$$\lim_{L \rightarrow \infty} R_L(x) = x - \sqrt{x^2 - 1}, \quad (\text{S14})$$

the Schwinger-Dyson equation (4) becomes

$$G(i\omega_n) = \left[\sqrt{-4t^2 - \omega_n^2} - \Sigma(i\omega_n) \right]^{-1}. \quad (\text{S15})$$

Note that $\sqrt{-4t^2 - \omega_n^2}$ is simply the $G^{-1}(i\omega_n)$ of a 1D chain. Unlike the SYK model, the coupling to the Majorana chain is relevant at small frequencies for $q > 2$, while the SYK $_q$ type of interaction is irrelevant for $q > 2$. Therefore, we consider SYK $_2$ where the interaction is marginal. To this end, we eliminate $\Sigma(i\omega_n)$ so that

$$G(i\omega_n) = \left[\sqrt{-4t^2 - \omega_n^2} - 2J^2 G(i\omega_n) \right]^{-1}. \quad (\text{S16})$$

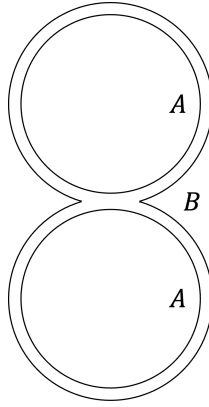
Solving it for the retarded Green's function gives

$$G(\omega - i\eta) = \frac{i}{4J^2} \left[\sqrt{4t^2 - (\omega - i\eta)^2} - \sqrt{4t^2 + 8J^2 - (\omega - i\eta)^2} \right]. \quad (\text{S17})$$

The associated spectral function is shown in Fig. 2(a).

For the interacting cases $q > 2$, we expand G using its spectral function $A(\omega)$ in Eq. (S17). This leads to the imaginary part of the retarded self-energies for any q in Eq. (5),

$$\Sigma''_q(\omega - i\eta) = J^2 \int \left[\prod_{i=1}^{q-2} \frac{d\nu_i}{\pi} A(\nu_i) \right] A \left(\omega - \sum_{j=1}^{q-2} \nu_j \right) \prod_{k=1}^{q-2} \left[n_F(\nu_k) - n_{\zeta_k} \left(\sum_{l=k}^{q-2} \nu_l - \omega \right) \right], \quad (\text{S18})$$



Supplementary Figure S1. The imaginary time contour for the second Rényi entropy. The fermionic field in a closed contour satisfies the conventional anti-periodic boundary condition, that leads to the fermionic Matsubara frequency.

where

$$n_{\zeta_i}(\nu) = \begin{cases} -n_B(\nu), & i \in 2\mathbb{Z}, \\ n_F(\nu), & i \in 2\mathbb{Z} + 1. \end{cases} \quad (\text{S19})$$

Hilbert transform of the spectral function recovers the full Green's function [71]. Numerical computations of the integrals can be formulated into convolutions that are expedited with the fast Fourier transform. For example, the self-energy of SYK₄ is given by convolutions in real frequencies which are denoted by $*$,

$$\Sigma_4''(\omega - i\eta) = \frac{J^2}{\pi^2} [(n_F A) * A * A + (\{(1 - 2n_F)A\} * A)\{1 + n_B\} * A]. \quad (\text{S20})$$

The local spectral function at the SYK₄ site is shown in Fig. 2(b)(c). Note that at high temperature, the Majorana chain-coupled SYK₄ dot behaves similarly to a 0+1D SYK dot. At low temperature, it flows away from the SYK point.

III. DERIVATION OF THE SECOND RÉNYI ENTROPY

To compute the Rényi entropy, we first assume that the chains satisfy an open boundary condition. Then, we divide the system into two regions, A and B. We are interested in the entanglement entropy between these two regions. The computation of entanglement entropy employs the replica trick [25]. Below, we first review the replica trick and then derive the Rényi entanglement entropy the 1+1D chains.

A. Review of the replica trick

We consider the thermal density matrix $\rho = \frac{e^{-\beta H}}{Z}$, $Z = \text{Tr}(e^{-\beta H})$. The second Rényi entropy of the region A is

$$S_2 = -\log \text{Tr}_A[(\text{Tr}_B \rho)^2] = -\log \frac{Z_{(2)}}{Z^2}. \quad (\text{S21})$$

Here, $Z_{(2)}$ denotes a path integral with a twist boundary condition on the region A. In terms of replica fields, the boundary condition reads

$$\psi_{j \in A}^{(1)}(\beta) = -\psi_{j \in A}^{(1)}(0), \quad \psi_{j \in A}^{(2)}(\beta) = -\psi_{j \in A}^{(2)}(0), \quad (\text{S22})$$

$$\psi_{j \in B}^{(1)}(\beta) = \psi_{j \in B}^{(2)}(0), \quad \psi_{j \in B}^{(2)}(\beta) = -\psi_{j \in B}^{(1)}(0), \quad (\text{S23})$$

where the superscripts 1, 2 denote the two replicas. The imaginary time contour for $Z_{(2)}$ is shown in Fig. S1. The fermionic field in a closed contour satisfies the conventional anti-periodic boundary condition that gives rise to the fermionic Matsubara frequency. A crucial point is that the closed imaginary-time contours of the fermionic fields in regions A and B have different

To make the result more versatile, we parametrize the hopping strengths between regions A and B by $r_{1,2}$ at the left and right interfaces, respectively. The hoppings to the SYK site from the left and the right are also parametrized by $q_{1,2}$, respectively. This extends our method to, e.g., the energy defect.

Discretizing imaginary time into an even number of points M , the sizes of the blocks $A_{1,2}$ are $K_{1,2}M \times K_{1,2}M$. Similarly, the sizes of $B_{1,2}$ are $L_{1,2}M \times L_{1,2}M$, and the sizes of $-i\omega - \Sigma$, $\pm it$ and $\pm it\sigma$ are all $M \times M$. The $\pm it$ blocks are proportional to identity in frequency space. The center block represents region A .

Denote the special matrices $(e_n)_{ij} := \delta_{i,n}\delta_{n,j}$. The determinant simplifies to

$$\begin{aligned} \det \mathcal{M} &= \det B_1 \det B_2 \det [A - r_1^2 t \sigma R_{L_1} \left(\frac{-i\Omega}{2t}\right) \sigma^\dagger e_1 - r_2^2 t \sigma R_{L_2} \left(\frac{-i\Omega}{2t}\right) \sigma^\dagger e_{K_1+K_2+1}] \\ &= \det B_1 \det B_2 \det A'_1 \det A'_2 \det \left[-i\omega - \Sigma_{(2)} - q_1^2 t^2 \left(A'_1\right)^{-1}_{K_1, K_1} - q_2^2 t^2 \left(A'_2\right)^{-1}_{1,1} \right]. \end{aligned} \quad (\text{S30})$$

Here we denoted $A'_1 = A_1 - r_1^2 t \sigma A_{L_1} \left(\frac{-i\Omega}{2t}\right) \sigma^\dagger e_1$, $A'_2 = A_2 - r_2^2 t \sigma R_{L_2} \left(\frac{-i\Omega}{2t}\right) \sigma^\dagger e_{K_2}$. The diagonal corner entries of A'^{-1} 's can be obtained from the formula [72]

$$\begin{bmatrix} A & B \\ C & D \end{bmatrix}^{-1} = \begin{bmatrix} (A - BD^{-1}C)^{-1} & 0 \\ 0 & (D - CA^{-1}B)^{-1} \end{bmatrix} \begin{bmatrix} \mathbf{1} & -BD^{-1} \\ -CA^{-1} & \mathbf{1} \end{bmatrix}. \quad (\text{S31})$$

This gives

$$\left(A'_1\right)^{-1}_{K_1, K_1} = \frac{1}{t} \frac{1}{-\frac{i\omega}{t} - \frac{1}{-\frac{i\omega}{t} - \frac{1}{\dots - \frac{1}{-\frac{i\omega}{t} - r_1^2 \sigma R_{L_1} \left(\frac{-i\Omega}{2t}\right) \sigma^\dagger}}}}. \quad (\text{S32})$$

In other words, let

$$\begin{aligned} \mathbf{D}_{0,L} &= r^2 \sigma R_L \left(\frac{-i\Omega}{2t}\right) \sigma^\dagger, \\ \mathbf{D}_{K,L} &= \left(-\frac{i\omega}{t} - \mathbf{D}_{K-1,L}\right)^{-1}. \end{aligned} \quad (\text{S33})$$

Note that when $\mathbf{D}_{0,L} = 0$, $\mathbf{D}_{K,L} = R_K \left(\frac{-i\omega}{2t}\right)$. The general formula is,

$$\mathbf{D}_{K,L} = \left[R_K \left(\frac{-i\omega}{2t}\right) - U_{K-2} \left(\frac{-i\omega}{2t}\right) \mathbf{D}_{0,L} U_{K-1}^{-1} \left(\frac{-i\omega}{2t}\right) \right] \left[1 - U_{K-1} \left(\frac{-i\omega}{2t}\right) \mathbf{D}_{0,L} U_{K-1}^{-1} \left(\frac{-i\omega}{2t}\right) \right]^{-1}. \quad (\text{S34})$$

Thus, $(A'_1)^{-1} = \mathbf{D}_{K_1, L_1}/t$. Similar results hold for $(A'_2)^{-1}$. Furthermore,

$$\det B_1 = t^{L_1} U_{L_1} \left(\frac{-i\Omega}{2t}\right), \quad (\text{S35})$$

$$\begin{aligned} \det A'_1 &= \det [A_1 - r_1^2 t \sigma R_{L_1} \left(\frac{-i\Omega}{2t}\right) \sigma^\dagger e_1] \\ &= t^{K_1-1} U_{K_1-1} \left(\frac{-i\omega}{2t}\right) \det [-i\omega - t R_{K_1-1} \left(\frac{-i\omega}{2t}\right) - r_1^2 t \sigma R_{L_1} \left(\frac{-i\Omega}{2t}\right) \sigma^\dagger] \\ &= t^{K_1-1} U_{K_1-1} \left(\frac{-i\omega}{2t}\right) \det [t R_{K_1-1}^{-1} \left(\frac{-i\omega}{2t}\right) - r_1^2 t \sigma R_{L_1} \left(\frac{-i\Omega}{2t}\right) \sigma^\dagger]. \end{aligned} \quad (\text{S36})$$

Therefore,

$$\begin{aligned} -\frac{I_{(2)}}{N} &= \frac{1}{2} \log \det [-i\omega - \Sigma_{(2)} - q_1^2 t \mathbf{D}_{K_1, L_1} - q_2^2 t \mathbf{D}_{K_2, L_2}] \\ &\quad - \frac{1}{2} \int d\tau_1 d\tau_2 G(\tau_1, \tau_2) \Sigma_{(2)}(\tau_1, \tau_2) + \frac{J^2}{4q} \int d\tau_1 d\tau_2 [2G(\tau_1, \tau_2)]^q \\ &\quad + \frac{1}{2} \log \det [t R_{K_1}^{-1} \left(\frac{-i\omega}{2t}\right) - r_1^2 t \sigma R_{L_1} \left(\frac{-i\Omega}{2t}\right) \sigma^\dagger] + \frac{1}{2} \log \det [t R_{K_2}^{-1} \left(\frac{-i\omega}{2t}\right) - r_2^2 t \sigma R_{L_2} \left(\frac{-i\Omega}{2t}\right) \sigma^\dagger] \\ &\quad + \frac{1}{2} \log \det [t^{L_1+L_2+K_1+K_2-2} U_{L_1} \left(\frac{-i\Omega}{2t}\right) U_{L_2} \left(\frac{-i\Omega}{2t}\right) U_{K_1-1} \left(\frac{-i\omega}{2t}\right) U_{K_2-1} \left(\frac{-i\omega}{2t}\right)]. \end{aligned} \quad (\text{S37})$$

The saddle point equations is

$$G_{(2)}^{-1} = -i\omega - \Sigma_{(2)} - q_1^2 t \mathbf{D}_{K_1, L_1} - q_2^2 t \mathbf{D}_{K_2, L_2}. \quad (\text{S38})$$

On the other hand, the untwisted action on a single replica can be obtained by modifying Eq. (S10),

$$\begin{aligned} -\frac{I}{N} &= \frac{1}{2} \sum_n \log \left[-i\omega_n - \Sigma(\omega_n) - q_1^2 t D'_{K_1, L_1} \left(\frac{-i\omega_n}{2t} \right) - q_2^2 t D'_{K_2, L_2} \left(\frac{-i\omega_n}{2t} \right) \right] \\ &\quad - \frac{1}{2} \int d\tau_1 d\tau_2 G(\tau_1, \tau_2) \Sigma(\tau_1, \tau_2) + \frac{J^2}{4q} \int d\tau_1 d\tau_2 [2G(\tau_1, \tau_2)]^q \\ &\quad + \frac{1}{2} \sum_n \log \left[t R_{K_1}^{-1} \left(\frac{-i\omega_n}{2t} \right) - r_1^2 t R_{L_1} \left(\frac{-i\omega_n}{2t} \right) \right] + \frac{1}{2} \sum_n \log \left[t R_{K_2}^{-1} \left(\frac{-i\omega_n}{2t} \right) - r_2^2 t R_{L_2} \left(\frac{-i\omega_n}{2t} \right) \right] \\ &\quad + \frac{1}{2} \sum_n \log \left[t^{L_1+L_2+K_1+K_2-2} U_{L_1} \left(\frac{-i\omega_n}{2t} \right) U_{L_2} \left(\frac{-i\omega_n}{2t} \right) U_{K_1-1} \left(\frac{-i\omega_n}{2t} \right) U_{K_2-1} \left(\frac{-i\omega_n}{2t} \right) \right], \end{aligned} \quad (\text{S39})$$

where $D'_{K,L}$ has the same recursive structure as $\mathbf{D}_{K,L}$, with $D'_{0,L} \left(\frac{-i\omega_n}{2t} \right) = r^2 R_L \left(\frac{-i\omega_n}{2t} \right)$. Since all terms commute, it can be simplified into

$$D'_{K,L} \left(\frac{-i\omega_n}{2t} \right) := \frac{1 - R_{K-1} \left(\frac{-i\omega_n}{2t} \right) r^2 R_L \left(\frac{-i\omega_n}{2t} \right)}{R_K^{-1} \left(\frac{-i\omega_n}{2t} \right) - r^2 R_L \left(\frac{-i\omega_n}{2t} \right)}. \quad (\text{S40})$$

The second Rényi entropy is given by $S_2 = I_{(2)} - 2I$. We can further simplify the expression by subtracting the zero S_2 when A and B are decoupled, thus dropping the last terms in (S37) and (S39). At $r = 0$, $\mathbf{D}_K = D'_K \left(\frac{-i\omega}{2t} \right) = R_K \left(\frac{-i\omega}{2t} \right)$. Denote the entropy terms in a decoupled system by \check{I} , and also let \check{G} be the Green's function G in (4) repeated on each replica, $\check{G} = G \otimes \mathbf{1}_2$, such that

$$\check{G}(\tau_1, \tau_2) = \begin{cases} G(\tau_1, \tau_2), & 0 \leq \tau_1, \tau_2 \leq \beta, \\ G(\tau_1 - \beta, \tau_2 - \beta), & \beta \leq \tau_1, \tau_2 \leq 2\beta, \\ 0, & \text{otherwise.} \end{cases} \quad (\text{S41})$$

we arrive at

$$\begin{aligned} S_2/N &= [I_{(2)} - 2I - (\check{I}_{(2)} - 2\check{I})] / N \\ &= -\frac{1}{2} \log \det \left[G_{(2)}^{-1} \check{G} \right] + J^2 \left(\frac{1}{4q} - \frac{1}{4} \right) \int d\tau_1 d\tau_2 \{ [2\check{G}(\tau_1, \tau_2)]^q - [2G_{(2)}(\tau_1, \tau_2)]^q \} \\ &\quad + \frac{1}{2} \log \det \left[\frac{1 - r_1^2 R_{L_1} \left(\frac{-i\omega}{2t} \right) R_{K_1} \left(\frac{-i\omega}{2t} \right)}{1 - r_1^2 \sigma R_{L_1} \left(\frac{-i\Omega}{2t} \right) \sigma^\dagger R_{K_1} \left(\frac{-i\omega}{2t} \right)} \right] + \frac{1}{2} \log \det \left[\frac{1 - r_2^2 R_{L_2} \left(\frac{-i\omega}{2t} \right) R_{K_2} \left(\frac{-i\omega}{2t} \right)}{1 - r_2^2 \sigma R_{L_2} \left(\frac{-i\Omega}{2t} \right) \sigma^\dagger R_{K_2} \left(\frac{-i\omega}{2t} \right)} \right]. \end{aligned} \quad (\text{S42})$$

Note that with trivial modifications, the last line is simply the entanglement between two 1+1D Majorana lattice with (possibly different) uniform nearest-neighbor hoppings.

IV. DERIVATION OF TRANSMISSION AND REFLECTION IN THE SYK DEFECT CFT

In this section, we derive the transmission and reflection coefficients for the SYK defect CFT. We first carry out coarse graining to obtain a continuum theory with the SYK defect, and then calculate the transmission and reflection coefficient from the two-point function of the stress tensor across the defect. Consider the free Majorana chain,

$$H = i2t \sum_r \psi_r \psi_{r+1}, \quad \{\psi_r, \psi'_r\} = \delta_{ij}. \quad (\text{S43})$$

After a Fourier transformation, it is easy to see that the Fermi momenta are located at $k_F = 0$ and $k_F = \frac{\pi}{a}$, where a denotes the lattice constant. Then, we take the following identification between the lattice fermion and the continuum fermion field

$$\begin{cases} \psi_{2r} = \sqrt{\frac{a}{2}} [\psi_R(x_r) + \psi_L(x_r)], \\ \psi_{2r+1} = \sqrt{\frac{a}{2}} [\psi_R(x_r) - \psi_L(x_r)], \end{cases} \quad r \in \mathbb{Z}, \quad x_r \equiv 2ra. \quad (\text{S44})$$

Here, $\psi_{R,L}(x)$ is the continuum fermion field operator with $\{\psi_L(x), \psi_L(x')\} = \{\psi_R(x), \psi_R(x')\} = \delta(x - x')$, and $\{\psi_L(x), \psi_R(x')\} = 0$. Thus, the unit cell is effectively doubled with the two low-energy chiral modes folded to $k = 0$. Note also that $\psi_L^\dagger = \psi_L$ and $\psi_R^\dagger = \psi_R$.

In terms of the continuum field, the Hamiltonian becomes

$$H = i \int dx v_F (\psi_R^\dagger \partial_x \psi_R - \psi_L^\dagger \partial_x \psi_L). \quad (\text{S45})$$

with $v_F = at$ and dropping the Umklapp terms.

For N decoupled Majorana chains, we can duplicate the theory with an additional index $i = 1, \dots, N$. Then we are ready to add the SYK interaction to the theory. Without loss of generality, consider the SYK site to be the even site at 0,

$$\sum_{jl} i J_{jl} \delta_{r,0} \psi_{r,j}^\dagger \psi_{r,l} = \sum_{jl} i J_{jl} a \delta(x) [\psi_{j,R}^\dagger(x) + \psi_{j,L}^\dagger(x)] [\psi_{l,R}(x) + \psi_{l,L}(x)] = \sum_{jl} i 2a \delta(x) \tilde{J}_{jl} \Psi_j^\dagger(x) P \Psi_l(x), \quad (\text{S46})$$

where $\Psi = (\psi_L, \psi_R)^T$, $P = \frac{1}{2} \begin{pmatrix} 1 & 1 \\ 1 & 1 \end{pmatrix}$, $\delta(x) = \delta(2ra) = \delta_{r,0}/2a$, and we have introduced the dimensionless coupling $\tilde{J}_{jl} = a J_{ij}$. Recall that J_{ij} is a Gaussian random variable with mean zero and variance given by (S3).

Combined with the free part, it leads to the following continuum theory

$$\mathcal{L}_E = \sum_j \Psi_j^\dagger(x) (\partial_\tau - i v_F \partial_x \sigma^z) \Psi_j(x) + \sum_{jl} i \delta(x) \tilde{J}_{jl} \Psi_j^\dagger(x) P \Psi_l(x). \quad (\text{S47})$$

Denoting $G := \frac{1}{N} \sum_i \langle \Psi_i \Psi_i^\dagger \rangle$, the large- N equation of motion reads

$$\begin{aligned} G(x, x'; \omega) &= G_0(x, x'; \omega) + G_0(x, 0; \omega) \Sigma(\omega) G(0, x'; \omega), \\ \Sigma(\omega) &= 2\tilde{J}^2 P G(0, 0; \omega) P. \end{aligned} \quad (\text{S48})$$

where $\tilde{J} = Ja$ with J being the strength of the variance defined in (S3). In the following, we set $v_F = 1$ for simplicity; in other words, $a = 1/t$ and $\tilde{J} = J/t$. Notice that we have performed disorder average to arrive at the equation of motion. The equation of motion is presented in mixed coordinates because the spatial translation symmetry is broken by the defect, whereas the temporal one is respected. This large- N equation of motion can be solved straightforwardly, leading to the solution:

$$\begin{aligned} G(x, y; \omega) &= G_0(x, y; \omega) + \frac{i \text{sgn}(\omega) (1 + \tilde{J}^2 - \sqrt{1 + 2\tilde{J}^2})}{4\tilde{J}^2} \\ &\quad \times \begin{pmatrix} (\text{sgn}(x) + \text{sgn}(\omega)(\text{sgn}(y) - \text{sgn}(\omega))) & -(\text{sgn}(x) + \text{sgn}(\omega)(\text{sgn}(y) + \text{sgn}(\omega))) \\ -(\text{sgn}(x) - \text{sgn}(\omega)(\text{sgn}(y) - \text{sgn}(\omega))) & (\text{sgn}(x) - \text{sgn}(\omega)(\text{sgn}(y) + \text{sgn}(\omega))) \end{pmatrix} e^{-(|x|+|y|)|\omega|} \end{aligned} \quad (\text{S49})$$

$$G_0(x, y; \omega) = i \left(\frac{\text{sgn}(\omega)}{2} + \frac{\text{sgn}(x-y)\sigma^z}{2} \right) e^{-|x-y||\omega|}, \quad (\text{S50})$$

which leads to the equal time correlation function

$$G(x, y) \equiv G(x, y; \tau = 0) = \frac{i\sigma^z}{x-y} + \frac{i(1 + \tilde{J}^2 - \sqrt{1 + 2\tilde{J}^2})}{2\tilde{J}^2(|x| + |y|)} \begin{pmatrix} -\text{sgn}(x) + \text{sgn}(y) & -\text{sgn}(x) - \text{sgn}(y) \\ \text{sgn}(x) + \text{sgn}(y) & \text{sgn}(x) - \text{sgn}(y) \end{pmatrix}. \quad (\text{S51})$$

The stress-energy tensor away from the defect is

$$T(x) = 2\psi^\dagger(x) P_R \partial_x \psi(x), \quad \bar{T} = -2\psi^\dagger(x) P_L \partial_x \psi(x), \quad (\text{S52})$$

where $P_L = \frac{1}{2}(1 + \sigma^z)$, and $P_R = \frac{1}{2}(1 - \sigma^z)$ are the projection to right and left movers, respectively. Using the full Green's

function, the correlation function of stress-energy tensor is given by

$$\langle T(x)T(-x) \rangle = -4\text{Tr} \left[P_R G^{(1,0)}(x, -x) P_R G^{(1,0)}(x, -x) \right] = \frac{\left(1 - \sqrt{1 + 2\tilde{J}^2}\right)^2}{4\tilde{J}^4(2x)^4}, \quad (\text{S53})$$

$$\langle \bar{T}(x)\bar{T}(-x) \rangle = -4\text{Tr} \left[P_L G^{(1,0)}(x, -x) P_L G^{(1,0)}(x, -x) \right] = \frac{\left(1 - \sqrt{1 + 2\tilde{J}^2}\right)^2}{4\tilde{J}^4(2x)^4}, \quad (\text{S54})$$

$$\langle T(x)\bar{T}(x) \rangle = 4\text{Tr} \left[P_R G^{(1,0)}(x, x) P_L G^{(1,0)}(x, x) \right] = \frac{\left(1 + \tilde{J}^2 - \sqrt{1 + 2\tilde{J}^2}\right)^2}{4\tilde{J}^4(2x)^4}, \quad (\text{S55})$$

$$\langle \bar{T}(-x)T(-x) \rangle = 4\text{Tr} \left[P_L G^{(1,0)}(-x, -x) P_L G^{(1,0)}(-x, -x) \right] = \frac{\left(1 + \tilde{J}^2 - \sqrt{1 + 2\tilde{J}^2}\right)^2}{4\tilde{J}^4(2x)^4}, \quad (\text{S56})$$

in which $G^{(1,0)}(x, y) \equiv \partial_x G(x, y)$ and $G^{(0,1)}(x, y) \equiv \partial_y G(x, y)$. Hence, the transmission and reflection coefficients are [14]

$$\mathcal{T} = \frac{\langle T(x)T(-x) \rangle + \langle \bar{T}(x)\bar{T}(-x) \rangle}{\langle T(x)T(-x) \rangle + \langle \bar{T}(x)\bar{T}(-x) \rangle + \langle T(x)\bar{T}(x) \rangle + \langle \bar{T}(-x)T(-x) \rangle} = \frac{2}{3 + \tilde{J}^2 - \sqrt{1 + 2\tilde{J}^2}}, \quad (\text{S57})$$

$$\mathcal{R} = \frac{\langle T(x)\bar{T}(x) \rangle + \langle \bar{T}(-x)T(-x) \rangle}{\langle T(x)T(-x) \rangle + \langle \bar{T}(x)\bar{T}(-x) \rangle + \langle T(x)\bar{T}(x) \rangle + \langle \bar{T}(-x)T(-x) \rangle} = 1 - \frac{2}{3 + \tilde{J}^2 - \sqrt{1 + 2\tilde{J}^2}}, \quad (\text{S58})$$

leading to the transmission coefficient presented in the main text.

V. DISCUSSIONS ON RÉNYI ENTROPY AND TRANSMISSION COEFFICIENT

A. Derivation of the transmission coefficient for energy defect in the Ising CFT

In this section, we briefly review the calculation of the transmission coefficient for an energy defect in the Ising CFT, i.e., the free Majorana model. We used a similar model as in the previous section to evaluate the transmission and reflection coefficient. In the presence of an energy defect, the continuum field theory reads

$$\mathcal{L}_E = \Psi^\dagger(x)(\partial_\tau - i\sigma^z \partial_x)\Psi(x) + g\delta(x)\Psi^\dagger(x)\sigma^y\Psi(x), \quad (\text{S59})$$

where g denotes the defect strength, and we set the Fermi velocity to be one for simplicity. Comparing this Lagrangian with the SYK defect (S47), the defect has a different form, and because the energy defect does not couple different flavors, we consider $N = 1$.

The scattering of the energy defect leads to the Schwinger-Dyson equation,

$$G(x_1, x_2; \omega) = G_0(x_1 - x_2; \omega) + G_0(x_1 - x_2; \omega)\Sigma(\omega)G_0(x_2; \omega) \quad (\text{S60})$$

$$\Sigma(\omega) = g \frac{\sigma^y}{1 - gG_0(0; \omega)\sigma^y}. \quad (\text{S61})$$

where $G = \langle \Psi\Psi^\dagger \rangle$ is the full propagator, and $G_0(x - y; \omega) = G_0(x, y; \omega)$ in (S50). Note that this Schwinger-Dyson equation is exact. The solution is

$$G(x_1, x_2, \tau_1, \tau_2) = \begin{pmatrix} \frac{i[4+g^2-2g^2(\Theta(x_1)\Theta(-x_2)+\Theta(-x_1)\Theta(x_2))]}{2\pi(4+g^2)(x_{12}+i\tau_{12})} & \frac{i2g(\Theta(x_1)\Theta(x_2)-\Theta(-x_1)\Theta(-x_2))}{\pi(4+g^2)(x_1+x_2+i\tau_{12})} \\ -\frac{i2g(\Theta(x_1)\Theta(x_2)-\Theta(-x_1)\Theta(-x_2))}{\pi(4+g^2)(x_1+x_2+i\tau_{12})} & -\frac{i[4+g^2-2g^2(\Theta(x_1)\Theta(-x_2)+\Theta(-x_1)\Theta(x_2))]}{2\pi(4+g^2)(x_{12}+i\tau_{12})} \end{pmatrix}, \quad (\text{S62})$$

where $x_{12} := x_1 - x_2$ and $\tau_{12} := \tau_1 - \tau_2$

With the full propagator, we can evaluate the transmission and reflection coefficient similarly to the previous section. The results are

$$\mathcal{T} = 1 - \frac{16g^2}{(4+g^2)^2}, \quad \mathcal{R} = \frac{16g^2}{(4+g^2)^2}. \quad (\text{S63})$$

This is consistent with Ref. [17].

B. Discussion on the effective central charge and the transmission coefficient

We discuss the relation between the transmission coefficient and the entanglement entropy. The entanglement entropy across the defect is given by an effective central charge \tilde{c}_n [26]

$$S_n = \frac{\tilde{c}_n(\mathcal{T})}{12} \left(1 + \frac{1}{n}\right) \log\left(\frac{L}{a}\right), \quad (\text{S64})$$

where S_n denotes Rényi- n entropy and a is the lattice constant. For von Neumann entropy, the effective central charge is [29]

$$\tilde{c}_1 = -\frac{6}{\pi^2} \{[(1+s)\log(1+s) + (1-s)\log(1-s)]\log s + (1+s)\text{Li}_2(-s) + (1-s)\text{Li}_2(s)\}, \quad s = \sqrt{\mathcal{T}}. \quad (\text{S65})$$

For the Rényi entropy, the results can be found in [31]. In particular, the Rényi-2 entropy calculated in our paper is

$$\tilde{c}_2(\mathcal{T}) = \frac{8}{\pi^2} \arcsin^2\left(\sqrt{\frac{\mathcal{T}}{2}}\right). \quad (\text{S66})$$

For the energy defect in the Majorana chain model, the transmission coefficient reads [29] $\sqrt{\mathcal{T}} = \frac{2}{1+g+1/(1+g)}$, where g is a parameter that captures the strength of the defect. In particular, for the Majorana chain model with a modified bond hopping studied in the main text, $g = (t' - t)/t$, with t (t') denoting the normal (defect) bond hopping strength. Note that the relation between the transmission coefficient derived from the continuum field theory (S63), and from the transfer matrix method is not straightforward. Nevertheless, they agree at the leading order as expected, since the continuum theory neglects higher-order contribution:

$$\mathcal{T} \approx 1 - g^2, \quad (\text{S67})$$

Therefore, the field theory calculation correctly predicts the leading behavior of the effective central charge

$$\tilde{c}_2 \approx \frac{1}{4\pi^2} - \frac{g^2}{2\pi^2}. \quad (\text{S68})$$

However, such a minimal consistency is violated for the SYK defect as discussed in the main text, as will be shown next.

In the interface geometry where $L_1 = K_2 = 0$, the Rényi-2 entropy in (S42) or (13) in the main text simplifies to

$$S_2/N = \frac{1}{2} \text{Tr} \log[G_{(2)} \tilde{G}^{-1}] + J^2 \left(\frac{1}{4q} - \frac{1}{4}\right) \int d\tau_1 d\tau_2 \{[2\tilde{G}(\tau_1, \tau_2)]^q - [2G_{(2)}(\tau_1, \tau_2)]^q\}. \quad (\text{S69})$$

To leading order in J at $q = 2$,

$$\frac{1}{2} \text{Tr} \log[G_{(2)} \tilde{G}^{-1}] = -\frac{1}{2} \text{Tr} \log[G_{(2)}^{-1} \tilde{G}] + J^2 \left(\frac{1}{4q} - \frac{1}{4}\right) \int d\tau_1 d\tau_2 \{[2\tilde{G}(\tau_1, \tau_2)]^q - [2G_{(2)}(\tau_1, \tau_2)]^q\}. \quad (\text{S70})$$

Let $\Gamma_{(2)} \equiv G_{(2)}|_{J=0} = (-i\omega - t\mathbf{D}_{K_1, L_1} - t\mathbf{D}_{K_2, L_2})^{-1}$ and $\tilde{\Gamma} \equiv \tilde{G}|_{J=0} = (-i\omega - t\mathbf{D}'_{K_1, L_1} - t\mathbf{D}'_{K_2, L_2})^{-1}$. Then

$$\begin{aligned} \frac{1}{2} \text{Tr} \log[G_{(2)} \tilde{G}^{-1}] &= \frac{1}{2} \text{Tr} \log \left[\frac{-i\omega - 2J^2 \tilde{\Gamma} - t\mathbf{D}'_{K_1, L_1} - t\mathbf{D}'_{K_2, L_2}}{-i\omega - 2J^2 \Gamma_{(2)} - t\mathbf{D}_{K_1, L_1} - t\mathbf{D}_{K_2, L_2}} \right] \\ &= \frac{1}{2} \text{Tr} \log \left[\frac{-i\omega - 2J^2 \tilde{\Gamma} - tR_{K_1} \left(\frac{-i\omega}{2t}\right) - tR_{L_2} \left(\frac{-i\omega}{2t}\right)}{-i\omega - 2J^2 \Gamma_{(2)} - tR_{K_1} \left(\frac{-i\omega}{2t}\right) - t\sigma R_{L_2} \left(\frac{-i\omega}{2t}\right) \sigma^\dagger} \right] \end{aligned} \quad (\text{S71})$$

$$\begin{aligned} &= \frac{1}{2} \text{Tr} \log \left[G_{(2)} \tilde{G}^{-1} (1 + 2J^2 \Gamma_{(2)} G_{(2)} - 2J^2 \tilde{\Gamma} \tilde{G}) \right] + O(J^4) \\ &= \frac{1}{2} \text{Tr} \log[\tilde{\Gamma}^{-1} \Gamma_{(2)}] + J^2 \text{Tr}[\Gamma_{(2)}^2 - \tilde{\Gamma}^2] + O(J^4). \end{aligned} \quad (\text{S72})$$

For the integral,

$$-\frac{3J^2}{4} \int d\tau_1 d\tau_2 \{[\tilde{G}(\tau_1, \tau_2)]^2 - [G_{(2)}(\tau_1, \tau_2)]^2\} = -\frac{3J^2}{4} \int d\tau_1 d\tau_2 \{[\tilde{\Gamma}(\tau_1, \tau_2)]^2 - [\Gamma_{(2)}(\tau_1, \tau_2)]^2\}. \quad (\text{S73})$$

Due to fermionicity, $\Gamma(\tau_1, \tau_2) = -\Gamma(\tau_2, \tau_1)$. Then $\text{Tr}(\Gamma^2) \equiv \int d\tau_1 d\tau_2 \Gamma(\tau_1, \tau_2) \Gamma(\tau_2, \tau_1) = -\int d\tau_1 d\tau_2 \Gamma(\tau_1, \tau_2)^2$. Thus,

$$\frac{S_2}{N} = \frac{S_2}{N} \Big|_{J=0} + \frac{J^2}{4} \int d\tau_1 d\tau_2 \{ [\tilde{\Gamma}(\tau_1, \tau_2)]^2 - [\Gamma_{(2)}(\tau_1, \tau_2)]^2 \} + O(J^4). \quad (\text{S74})$$

Therefore, the leading order change in S_2 and hence \tilde{c}_2 is J^2 . However, from Eq. (S57) or (16) in the main text, $\mathcal{T} = 2 / (3 + \tilde{J}^2 - \sqrt{1 + 2\tilde{J}^2}) \approx 1 - J^4/2$. Consequently, the leading-order change in $\tilde{c}_2(\mathcal{T})$ is J^4 , in disagreement with that extracted from the scaling of S_2 , as plotted in Fig. 4(d) in the main text.

Finally, we address the independence of the g -function on J in the thermodynamic limit. In the setup to compute the g -function, $K_1 = K_2 = K$ and $L_1 = L_2 = L$. When K is large, $\lim_{K \rightarrow \infty} \mathbf{D}_{K,L} = \lim_{K \rightarrow \infty} D'_{K,L}(\frac{-i\omega}{2t}) = \lim_{K \rightarrow \infty} R_{K+L}(\frac{-i\omega}{2t})$ for low-frequency components. In this case, the defect is too far from the interface to affect each other. Thus, $G_{(2)} \approx \tilde{G}$. As a result, S_2 comes only from noninteracting chains. In contrast, when the defect is next to the interface, e.g., $K_2 = 0$ as in (S71), the twist operator is immediately present in $G_{(2)}$, so its effect survives in the thermodynamic limit.